


RESEARCH ARTICLE

Manifestation of lattice topology data model for indoor navigation path based on the 3D building environment

Syed Ahmad Fadhli Syed Abdul Rahman ¹, Khairul Nizam Abdul Maulud^{2,3,*}, Biswajeet Pradhan^{4,5} and Sharifah Nurul Ain Syed Mustorpha⁶

¹Cadastral Division, Department of Survey and Mapping Malaysia, 50578 Kuala Lumpur, Malaysia;

²Department of Civil Engineering, Faculty of Engineering & Built Environment, Universiti Kebangsaan

Malaysia, 43600 UKM Bangi, Selangor, Malaysia; ³Earth Observation Centre, Institute of Climate Change (IPI),

Universiti Kebangsaan Malaysia, 43600 UKM Bangi, Selangor, Malaysia; ⁴The Centre for Advanced Modelling

and Geospatial Information Systems (CAMGIS), Faculty of Engineering and Information Technology,

University of Technology Sydney, Sydney, NSW 2007, Australia; ⁵Department of Energy and Mineral Resources

Engineering, Sejong University, Choongmu-gwan, 209 Neungdong-ro, Gwangjin-gu, Seoul 05006, Korea and

⁶Centre of Studies for Surveying Science and Geomatics, Faculty of Architecture, Planning and Surveying,

Universiti Teknologi MARA, 40450 Shah Alam, Selangor, Malaysia

*Corresponding author. E-mail: knam@ukm.edu.my

Abstract

Navigation, also known as discovering one's direction, is a complex human activity. To produce effective routes, it relies on knowledge of the surroundings' precise geometry and semantic information. Complex geometrical data can be precisely delineated with the improvement of 3D geometric models. A precise 3D geometric model containing a specifically built-in Building Information Modelling (BIM) environment can be integrated into the Geographical Information System platform for indoor path generation to satisfy the requirements of indoor location-based services. Therefore, this paper proposes an approach to evaluate a 3D indoor topology network called a lattice topology data model (LTDM) for the floor-level paths in a 3D multipatch-based model. The LTDM requires the geometric information of the integrated BIM model to identify the indoor space and bounding lines for indoor network generation. The novelty of this study is in the application of the replacement of cell values into vector length for pathfinding through a combination of the Poincaré duality theorem and Dijkstra's algorithm. The Campus Infrastructure Building model was chosen to validate the proposed method. Multiple space centroid pairs within the floor level were randomly selected to identify the shortest path using the LTDM principle. Paths drawn from the Medial Axis Transformation were compared with LTDM-generated paths for availability testing. The average floor-level path availability was 112% due to the generation of extra paths reflecting real-life situations. The LTDM paths were compared with on-site measurements for accuracy tests, and the average error rate was 3.18%. The results show that the implementation of the LTDM generates an excellent topology data network.

Keywords: LTDM; lattice; spatial analysis; topology; indoor navigation path

Received: 12 June 2021; Revised: 2 August 2021; Accepted: 12 August 2021

© The Author(s) 2021. Published by Oxford University Press on behalf of the Society for Computational Design and Engineering. This is an Open Access article distributed under the terms of the Creative Commons Attribution-NonCommercial License (<https://creativecommons.org/licenses/by-nc/4.0/>), which permits non-commercial re-use, distribution, and reproduction in any medium, provided the original work is properly cited. For commercial re-use, please contact journals.permissions@oup.com

1. Introduction

The use of 3D spatial information to describe physical and human landscapes in urban environments has wide applications in multiple fields of geo-science (Sazandeh *et al.*, 2018). Some of these focus on 3D land use planning (Yépez Rincón & Lozano García, 2017), monitoring environments (Stoter *et al.*, 2020), cadastre planning (Shin *et al.*, 2020), and urban simulations (Abdul Rahman *et al.*, 2021). Most of these analyses embraced real-life conditions by analysing highly detailed levels of spatial information in specific areas, such as emergency management systems (Chen *et al.*, 2020), transportation (Chang *et al.*, 2015; Fonseca *et al.*, 2017), and indoor environmental monitoring (Abd Malek *et al.*, 2018; Cheliotis, 2020). Integrating 3D capabilities and functionalities is essential to demonstrate a 3D environmental structure and steer 3D-based spatial analyses (Lee & Yo, 2021). Therefore, extensive research has been conducted to devise and develop functional 3D GIS data structures and operations for 3D analysis (Matarneh *et al.*, 2019). Since the GIS platform only supports the 3D boundary representation (B-rep) model (Abou Diakité & Zlatanova, 2016), the development of 3D spatial analysis focuses on 3D B-rep, which is an extension of the representation of planar configurations in 2D B-rep.

As positioning technology evolves, location-based services (LBSs) also diversify from outdoor to indoor environments (Lin & Lin, 2018). Unfortunately, although available outdoors, the implementation of LBS through GPS for indoor maps is insufficient because of the limitations of positioning accuracy (Mortari *et al.*, 2014; Sita-Nowicka & Fotheringham, 2019). Since the main output of an indoor positioning simulation is to represent the actual on-the-ground situation and find the most effective path for users, the identification of ideal navigation path criteria has become central to current research (Gülgen, 2016; Imottesjo & Kain, 2018). Li *et al.* (2010) mentioned that using a grid graph-based representation, the model considers the urban environment as a frame of reference at various levels of granularity. The gradual transition has the advantage of combining structural and topological properties and indirectly accounting for the metric of volume, which current indoor space models frequently ignore.

In the literature, many indoor topologies have been developed to provide better results in indoor navigation activities (Kim & Kim, 2019; Singh *et al.*, 2019). Three existing graph-based models are mainly used in indoor navigation, namely visibility graphs (Pang *et al.*, 2019), straight skeletons, and Generalized Voronoi Graphs (GVGs; Pang *et al.*, 2019). The visibility graph comprises paths formed by a set of commonly visible points. Unfortunately, the visibility graph path direction is not suitable to human cognizance of a path (Mortari *et al.*, 2014), and does not control the number of generated nodes and affects the number of edges generated (Yang & Worboys, 2015). On the other hand, straight skeletons are intended to seize the medial axis of a geometric shape by altering the polygon into a network structure. Unfortunately, for the building with irregular spaces, the straight skeleton generates many unnecessary nodes and bending paths, leading to poor results. For the GVG, it is gained from the generalization of generalized Voronoi Diagram where the curve path is replaced by the straight path and based on the building boundary (such as walls) as the borderline (Lin & Lin, 2018). Unfortunately, it downgrades the precise geometric data since the output is modified and affects the results compared to real-life applications. This can be seen where most of them focus on topology's connection but neglect the positioning and physical factors such as building orientation and the on-site accessible path and

spaces (Liu, 2017), which is fundamental to represent the actual on-the-ground situation.

Therefore, this study reinvented and evaluated the indoor topology developed by Li *et al.* (2010), which utilized a grid graph-based representation of the 2D environment for 3D indoor topology, namely the lattice topology data model (LTDM) for the 3D environment. The purpose of the LTDM is to create indoor navigation for the floor-level path of the 3D BIM model in the GIS platform and present this through a 3D environment based on a 2D grid graph-based model. The LTDM uses the Poincaré duality theorem and Dijkstra's algorithm to interpret the topological terms and combine them with the lattice network to identify the most suitable paths for users. Since the Medial Axis Transformation (MAT) algorithm is widely used in the indoor network, distances from the LTDM were compared with the results from the MAT algorithm to determine which method offers users the most precise and flexible approach.

2. Literature Review

This section describes several essential aspects: GIS, BIM, spatial data, lattice data, the MAT, and the Poincaré duality theorem.

2.1. Geographical information system (GIS) and building information modelling (BIM)

GIS is popularly known for its technology to understand geography and make intelligent decisions (Teo & Cho, 2016; Rahman *et al.*, 2020). GIS works by manipulating geospatial data to allow users to read a map and select the data needed for a particular project or task. It can also plot relationships between data, patterns, and trends in maps, reports, and charts. GIS offers flexibility to users to perform various management tasks, such as space management, visualization, planning, emergency response, and various other applications (Dou *et al.*, 2020; Abdul Maulud *et al.*, 2021; Aldhshan *et al.*, 2021).

BIM is a digital system that represents building information and uses it as an object-oriented approach to describe features and the behaviour of each building information (Zhu *et al.*, 2018). BIM offers a flexible approach that includes all the essential elements for a particular model design phase. Several elements encompass the overall design, construction, and post-construction processes in the architectural and engineering industries. BIM and GIS can complement each other through integration (Zhu *et al.*, 2018). GIS helps BIM connect to the external environment, and BIM's capabilities extend the scope of GIS to the internal environment. This combination can achieve more benefits by working together than working separately. In this study, the 3D BIM model with Level of Details 4 (LOD4) was selected as a base model due to it has excellent visualization and accuracy in dimension (Abou Diakité & Zlatanova, 2016). Besides that, the internal structure of the building also needs to be considered, which the LOD4 are vital to represent the actual on-the-ground situation.

2.2. Spatial data

Two approaches can be utilized to display grid-based data: the grid and the lattice (Zhou *et al.*, 2018). The grid structure utilizes cell forms to configure the surface. The 2D form fills every cell with representative values of the contour interval, while the 3D adaptation pushes every cell up to its relative elevation (Joseph, 2002; Rahimi & Malek, 2015). The lattice structure utilizes lines to

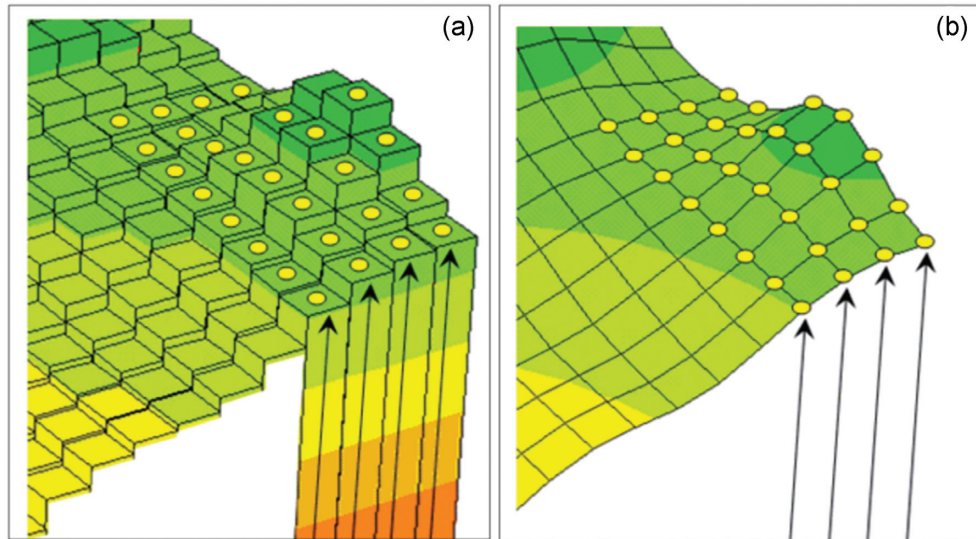


Figure 1: Difference between (a) grid-based and (b) lattice-based data (modified after Joseph, 2002).

convey the surface arrangement. The 2D form distinguishes the breakpoints for the equivalent interval of the increasing height of contour lines. For the 3D form, each line intersection is extruded to the general stature of the elevation value as recorded for each location. This study transforms the lattice structure from the concept of grid-based data (based on cell value) into vector-based data (based on line value). The lattice represents the line features in the network and connects appropriately to form a navigation network. The difference between grid-based data and lattice-based data can be seen in Fig. 1.

2.3. Lattice data, the MAT, and the Poincaré duality theorem

A lattice network in the grid-based principle signifies the surface by utilizing various similarly dispersed sample points, known as mesh points, which refer to a common origin (Zhen et al., 2020). The specimen distance is continuous in the x and y directions. Each specific position for the z value between lattice mesh points can be estimated by standard interpolation based on neighbouring mesh points. A 3D grid transforms the data model by allocating each cell with an equal attribute value. As mentioned above, this study utilized lattice data in the form of a vector-based principle (a line features network) in which each mesh point was transformed into the intersections of lattice line features that fit the coordinate values in a 3D environment. The line features act as a ‘railway’ for path navigation and fit perfectly with the application of Dijkstra’s algorithm.

One example of an algorithm based on the ‘railway’ is known as the Medial Axis Transform (MAT). The MAT principle has been applied in various ways, such as Straight-Medial Axis Transform (S-MAT), developed by Lee (2004). The concept is based on a bisecting line. An example can be explained using a rectangular space, where the first step is to generate a bisecting line between the interior vertex of the space. After that, from the intersection of the bisecting line, it is subsequently associated with forming a skeleton containing one backbone (node) and four ribs (edges). Although it is a space with a simple and reasonably regular shape, it can give outstanding results regarding the navigation network. Further proposals were made to improve the S-MAT method through the Modified-Medial Axis Transforma-

tion (M-MAT) by Taneja et al. (2016). They found that the M-MAT was capable of applying a Type-I corridor, which S-MAT cannot. Unfortunately, for buildings with irregular spaces, the straight skeleton generated many unnecessary nodes and bending paths that led to poor results.

Improving the complex spatial connections between 3D objects is essential; therefore, this paper utilized Poincaré Duality to interpret the topological terms. The Poincaré Duality was selected due to its capabilities in deriving the topological relationships between a set of 3D characters (Lee et al., 2016). The connectivity between nodes through vector lines in topology is fundamental in the GIS navigation process (Liu, 2017). A graph in elementary space is reformed into a dual graph in double space, dependent on specific procedures. In 2D environments, 2-cells, 1-cell, and 0-cell in elementary space were changed into 0-cell, 1-cell, and 2-cells separately in double space. On the other hand, corresponding cells in 3D space were 3-cells to 0-cell, 2-cells to 1-cell, 1-cell to 2-cells, and 0-cell to 3-cells (Lee et al., 2016). The spatial relationships between 3-cells are indicated by the duality changes of 3-cells to 0-cell and 2-cells to 1-cell (Fig. 2).

3. Indoor Environment Replication

3.1. Generation of indoor spaces

The fundamental principle for generating an indoor network using the LTDM is to classify the indoor spaces for each floor. Figure 3 diagrams the workflow for this phase of the study. First, the LTDM read a 3D BIM model that was integrated with a GIS platform using a multipatch shapefile (.shp) format, according to a method suggested by Abdul Rahman and Abdul Maulud (2019). The suggested technique uses a Feature Manipulation Engine (FME) as a medium to extract the relevant features needed to generate the indoor network, such as walls, columns, and doors. The FME Revit Plug-in extension is needed to integrate a BIM 3D model from Revit into the 3D GIS model. The integration process from *.rvt data format to *.rvz data format can be conveniently translated by allowing the extension and defining several items of specification information for the transformations, such as the LOD (low, medium, and height) and the property collection (base quantity and common property set). After the model has been

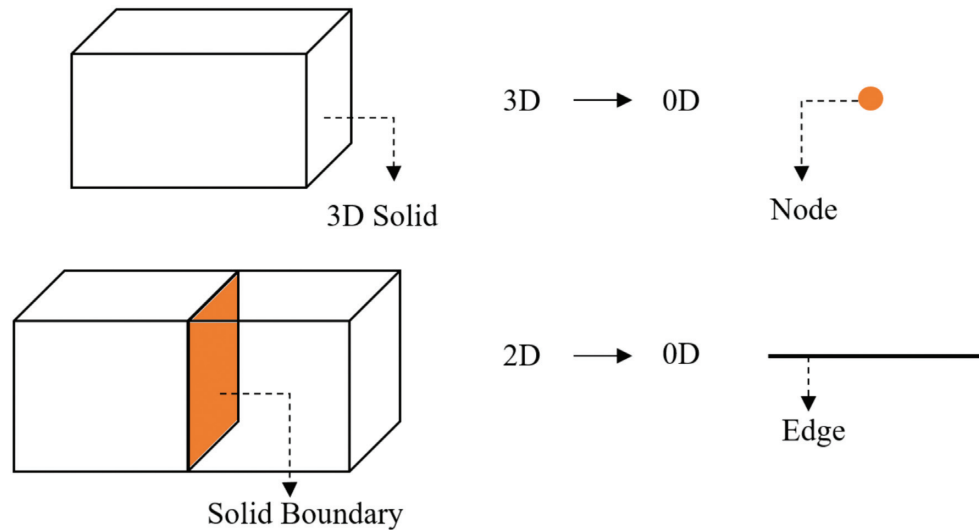


Figure 2: Poincaré Duality interpretation of topological terms.

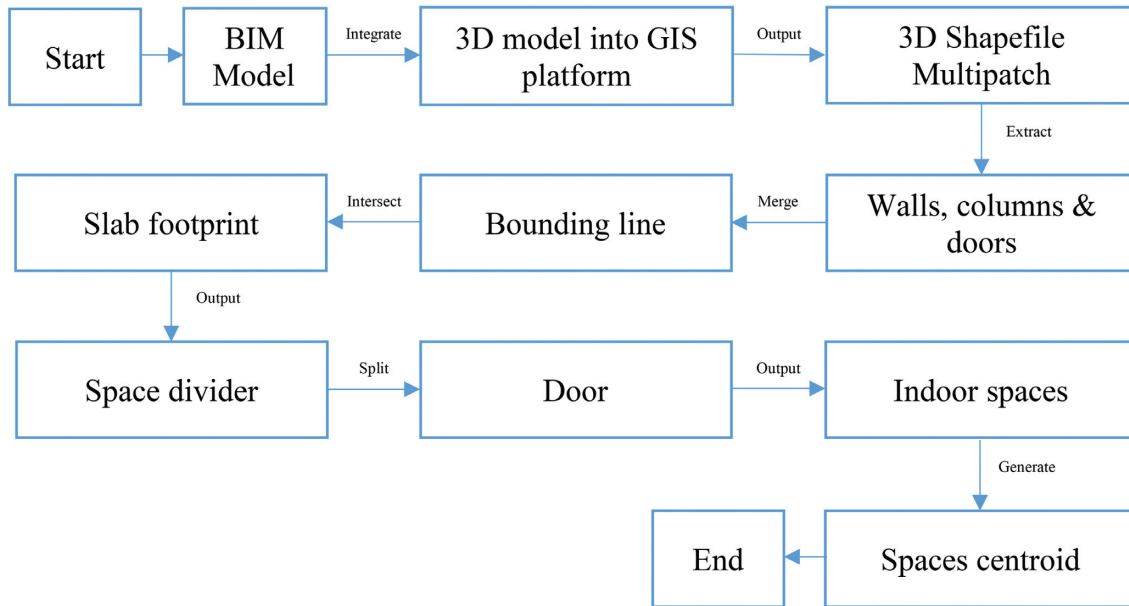


Figure 3: Flow chart showing generation of indoor spaces.

converted to *.rvz, a workspace must be specified (reader feature type or writer feature type). Since the target data format is Multipatch Geometry, the writer format must be set to ESRI Shapefile, and the reader data format must be set to Autodesk Revit. When the workspace is confirmed, the integration process can be started and all the data are stored within a GIS Geodatabase. The classification of indoor spaces in a GIS environment is essential because the indoor spaces generated by BIM include the spaces under the wall. Therefore, the new indoor spaces exclude spaces under the wall that need to be generated to avoid navigation complications.

Next, the merging process occurs to create bounding lines (red lines in Fig. 4). These bounding lines are used as dividers to separate the indoor spaces within the building. Consequently,

the bounding lines intersect with the slab footprint, as shown in Fig. 4, and split the door lines to create the indoor spaces based on the slab footprint.

The indoor spaces generated in this way are classified into cabins, corridors, and inaccessible spaces. Cabins represent spaces that are generally used as offices. A corridor is defined as a space connecting cabins and an inaccessible space, defined by its inability to accommodate navigation activities. From the indoor spaces generated, it can be seen (Fig. 5) that space centroids (0D) occupy the centre of each indoor space using Poincaré Duality, as explained in Section 2.3. These space centroids are essential because they form the main nodes that become the first determinant of indoor navigation through connected arcs (1D).

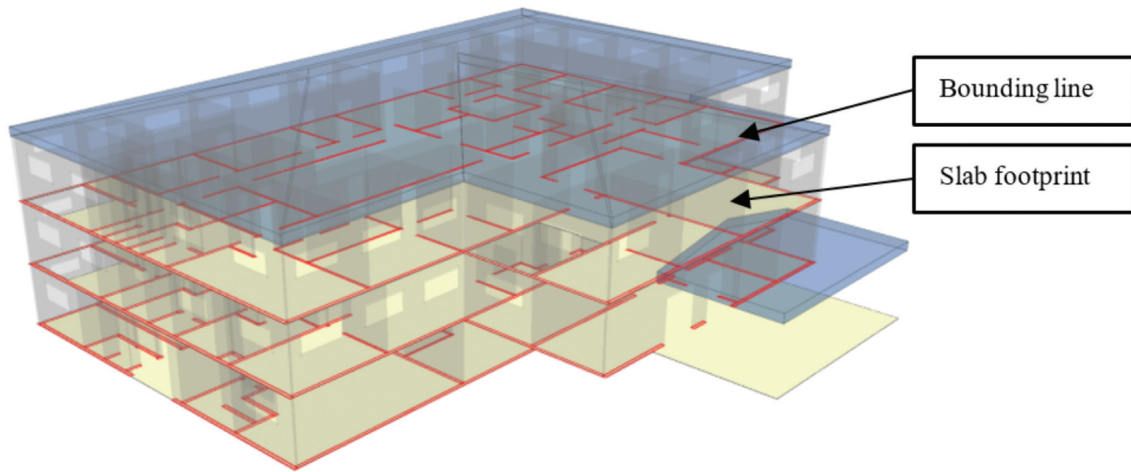


Figure 4: Bounding lines (red line).

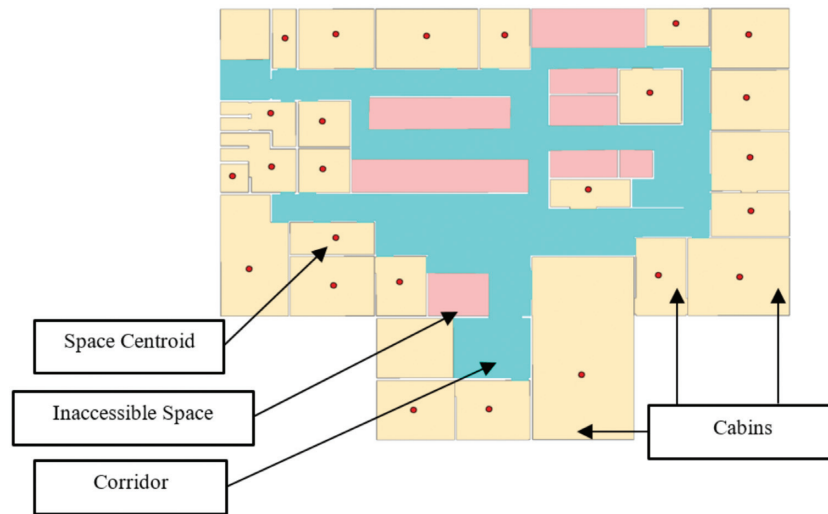


Figure 5: Types of indoor components.

3.2. Generation of floor-level paths

The network of indoor networking must connect with every accessible part of the floor, including rooms, corridors, and transition areas such as lobby floors. It is essential to understand that the network should not be overgeneralized because it is expected that some parts of the indoor building may not be navigable (Mortari *et al.*, 2014; Lee *et al.*, 2017). Although the network must not be overgeneralized, that does not mean that the paths should be unreasonably dense. Too many unnecessary paths would minimize the potential of the paths as a guiding tool and increase the computing time needed for the system to produce the most effective path.

Figure 6 shows the LTDM flowchart for producing floor-level paths to fit the 3D environment. Four main features (buildings, walls, floors, and spaces) were involved in the output model, based on the Poincaré Duality, in the topology of adjacency to generate the topology of connectivity (Fig. 7). Building features become the frame for data, which in the Poincaré Duality concept is known as Spaces (Primal and Dual). The walls and spaces are defined as cells, where each cell is differentiated based on the function of the restriction and zones of the generated con-

nective topology. Lastly, floors were used as a benchmark for the z-values (3D height) in establishing the lattice network. The process then continued with the restriction specifications for the 3D model and the lattice specifications for creating an effective network path. All the procedures conducted within the ArcGIS Pro Geodatabase environment and the generated lattice were saved in the Geodatabase. This study used the ArcGIS Pro as a platform because of its capabilities in conducting analysis, visualizing, and synchronizing 2D and 3D data simultaneously (Abdul Rahman & Abdul Maulud, 2019; Zhu & Wu, 2021). It also provides Geodatabase to store multiple 3D data structures such as 3D model (in 3D multipatch structure) and generated lattice (in 3D vector line structure) for analysis.

3.2.1. Restriction parameters

Two categories of restriction parameters were used in this study: space and line restriction parameters (Li *et al.*, 2010). The space restriction parameter focused on restraining the space features and erasing certain parts of the network because not all spaces are required for path consideration. An example used in this study is that of stairs and office space. Stairs were set as a space

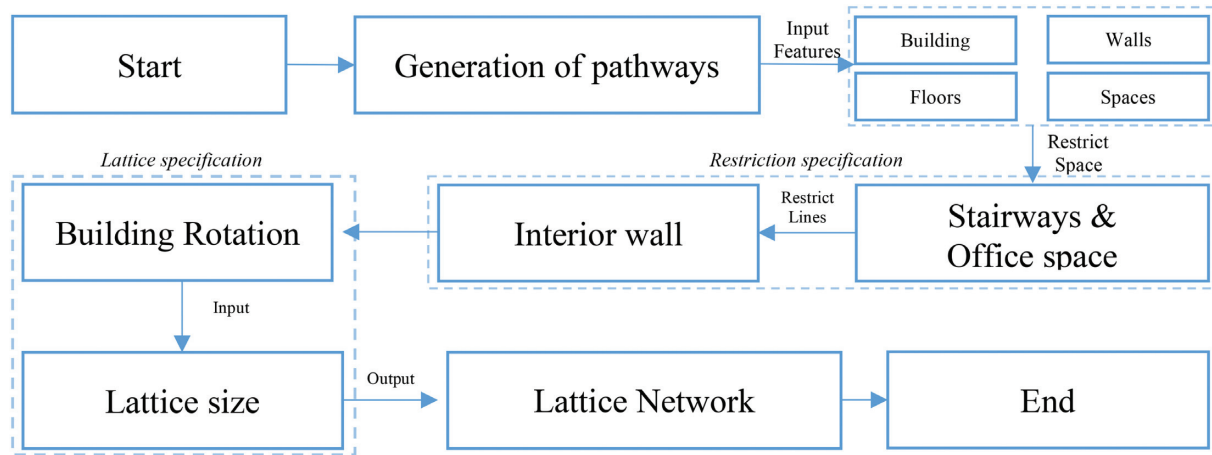


Figure 6: Flowchart showing generation of floor-level paths.

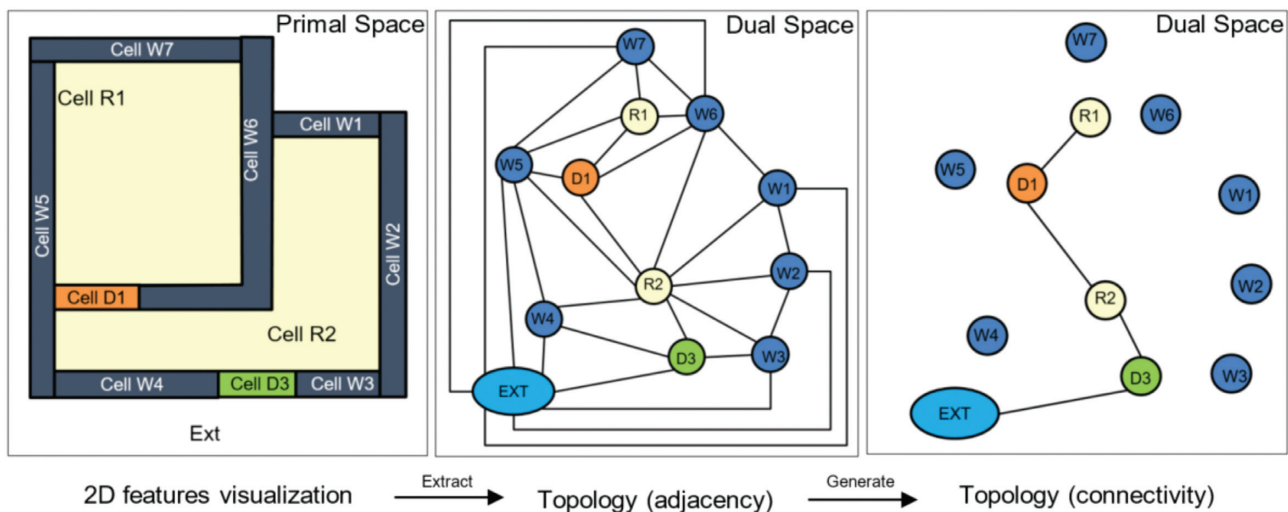


Figure 7: Poincaré Duality extraction (Lee et al., 2016).

restriction parameter because this study focused exclusively on floor-level paths. However, stairs were retained for consideration in producing pathways. Office space is set as a restriction parameter due to furniture within partitions, whereby office space is typically not used as a user's path, as Ergan et al. (2018) highlighted. By eliminating these spaces, the lattice generated is reduced and given a minimum space option for creating a network path that is effective for the user. Restricted spaces are labelled as inaccessible spaces in Fig. 5.

The line restriction parameter function is related to restraining the lattice boundary used to limit the generated network. An example used in this study is the interior wall. The physical boundaries of the interior wall include columns, furnishings, and so on, representing line features of walls. These line parameters were used as indicators to determine the distance to the nearest wall and ensure the generated lattice has some gaps within the interior walls. By highlighting this parameter, the lattice generated is maintained within the building spaces without physical contact with the interior wall, leading to efficient network path results. The line restriction parameter is based on the wall features, as shown in Fig. 4, known as the bounding line.

3.2.2. Lattice parameter

Constructing a floor-level path using the LTDM made the lattice the foundation for network generation in this study. This method generated a lattice for each indoor space (cabins and corridors) and connected it with the space centroid to form the paths, as shown in Fig. 8. The parameter utilized in this study comprised two main elements: the lattice rotation parameter and the lattice size parameter.

One of the requirements of generating a lattice is that the lattice rotation is based on the cardinal angular direction. With an unfit rotation, the distance between edges can be different at the beginning and the end with the same nodes, as shown in the example in Fig. 9. The implementation of Dijkstra's algorithm without the precise rotation value would significantly impact the results of indoor navigation. Dijkstra's algorithm concept will be explained in Section 3.3. Here, the lattice rotation used was $55^{\circ}34'16''$ since this is the actual cardinal direction of the Campus Infrastructure Building (CIB) towards the north (Fig. 10), which was measured using the land survey method. The actual cardinal direction is essential when the modelling implementation is based on BIM-GIS modelling, whereby spatial information becomes a fundamental modelling aspect.

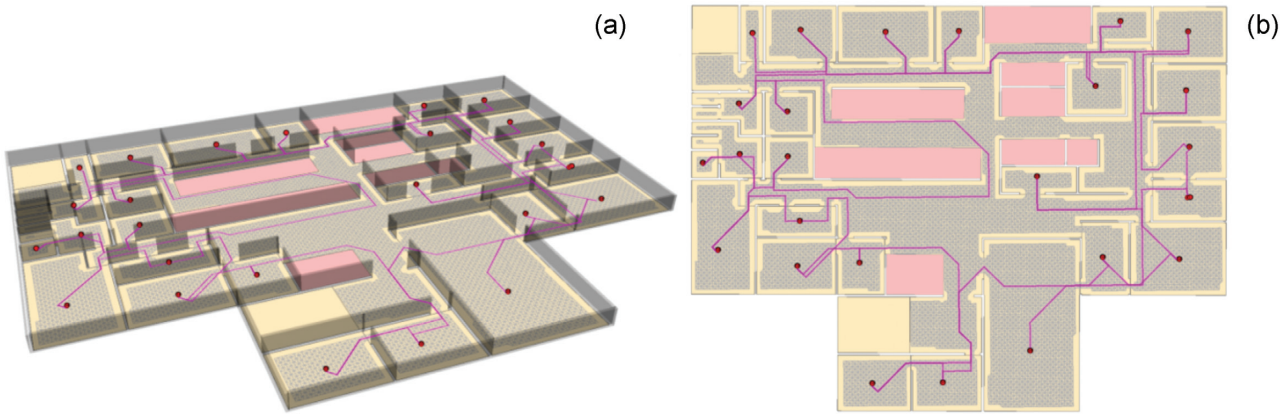


Figure 8: Lattice and network path connectivity in (a) 3D and (b) plan view.

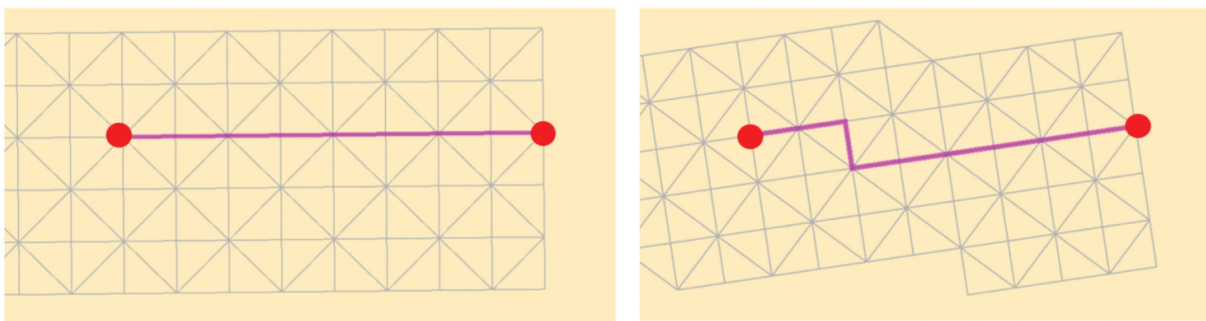


Figure 9: Different path distances due to unfit lattice rotation.

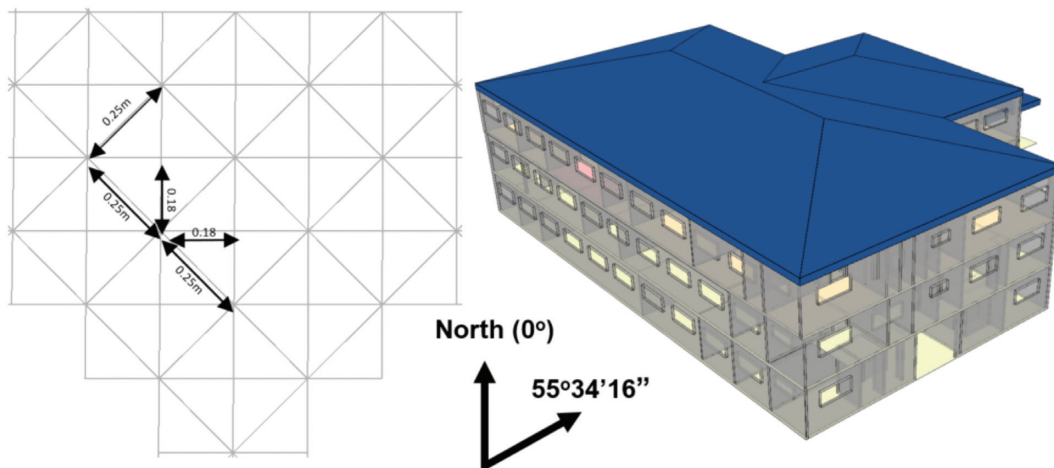


Figure 10: Lattice size 0.250 m with 55°34'16'' rotation.

Choosing the ideal lattice size for a building was fundamental to this study. If it were too large, the lattice would not fit through narrow entryways. If it were too small, the dataset would be unreasonably large, and the time needed for the route calculation would surge. In this study, the access width was tested to become the factor used to identify the most suitable lattice size. The access points are separated into three categories: door access, open access, and partition access (Table 1). Door access is defined as a path used to access a specific room or enclosed space. Open access is described as a narrow side

Table 1: Types and numbers of access points.

Access type	Floor level			Total
	Level 1	Level 2	Level 3	
Door access	20	30	29	79
Open access	1	3	2	6
Partition access	2	4	7	13
Total	23	37	38	98

Table 2: The number of accesses of each width.

Access width (m)	Floor level			Total	Percentages (%)
	Level 1	Level 2	Level 3		
0.800	3	3	3	9	9.184
0.950	10	25	27	62	63.265
1.200	1	2	2	5	5.102
1.500	1	0	3	4	4.082
1.700	8	4	2	14	14.286
1.930	0	3	1	4	4.082
Total	23	37	38	98	100.00

```

Input:    G (V,E)
Output:  S
Procedure: Dijkstra(G, root)
// initialisation
foreach vertex v in G:
  dist(v) ≤ Inf // dist(v) indicates the shortest distance between root and v
  prev(v) ≤ Undef
end for
// maintain the closest vertex to the source
dist(root) ≤ 0
while V is not empty:
  v ≤ vertex in V with minimal distance value
// the algorithm trails the vertex that is closest to root and uses it as the new frontier to extend the path
remove v from Q
for child w of v:
  dist ≤ dist(v) + weight(v, w)
  if (dist < dist(w)):
    dist(w) ≤ dist
    prev(w) ≤ v
  end if
end for
end while
END

```

Figure 11: Dijkstra's algorithm pseudo-codes.

along a corridor, and partition access is a narrow path between partitions. This factor is vital because some paths have smaller widths than a standard size door.

There are six main widths for doors and accesses in the building: 0.800, 0.960, 1.200, 1.500, 1.700, and 1.930 m. Each level has a different quantity of access points. Next, 0.950 m was selected as the weight to identify a suitable lattice size by differentiating the values into $5/19 W$, $1/4 W$, $1/3 W$, $1/2 W$, and W . This is because a width of 0.950 m is the most common size, representing 63% of the total number of accesses (Table 2) for all three levels. The weight of $5/19 W$ (0.250m) was tested because it is recognized as an ideal lattice size for a standard size building (Akram & Tamera, 2019). In this study, a lattice size of $1/3 W$ or 0.380 m was selected as the most suitable size. The details are discussed in Section 4.2.

3.3. Classification

After undergoing several processes, as shown in Fig. 6, the lattice network was generated (see example in Fig. 8). Based on the nodes generated using Poincaré Duality, the start and end nodes for navigation could be set up, and the edges could use the lattice as the medium. Figure 11 presents the pseudo-codes for Dijkstra's algorithm used to find the shortest path based on Poincaré Duality.

The pseudo-codes were based on $G = (V, E)$, where G is for weighted graph, V is for vertices (spaces centroid, 0D), and E is for edges (arcs, 1D). Pseudo-codes addressed the algorithm complexity, resulted from the relationship between the numbers of nodes, the distance from the edges, and the number of edges. Based on the lattice network, a network path

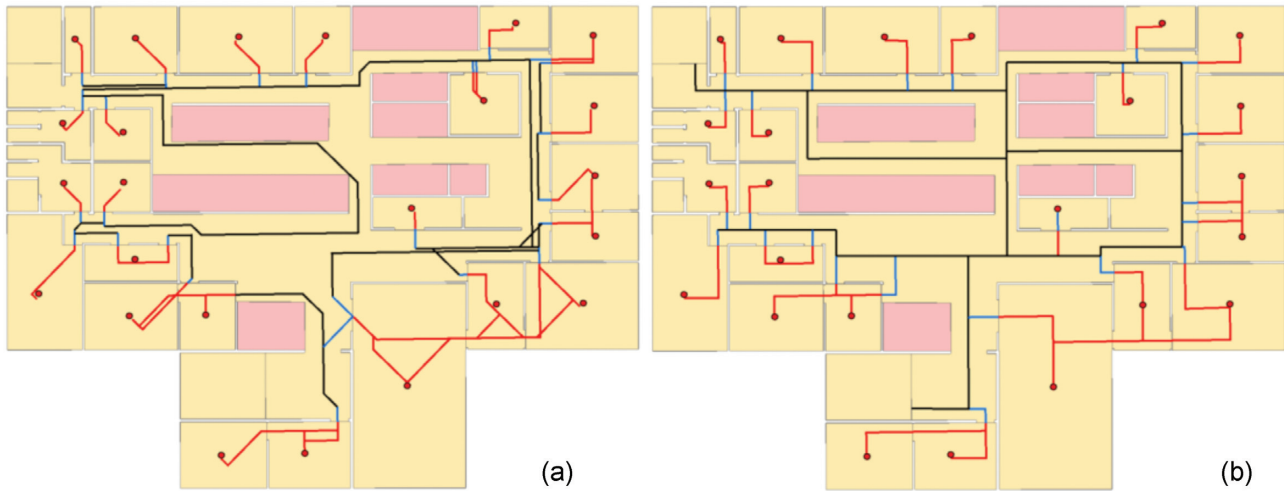


Figure 12: Path classification (a) LTDM and (b) MAT.

Table 3: Availability testing summary.

Floor	1st Floor		2nd Floor		3rd Floor	
	LTDM	MAT	LTDM	MAT	LTDM	MAT
Principle Lattice size (m)	0.250 m		0.237 m		0.380 m	
Indoor spaces	20	20	36	36	36	36
Inside-corridor paths	3	3	17	14	16	13
Access-to-corridor	13	13	24	24	26	26
Access-to-cabin	17	16	27	24	36	24
Floor-level paths	33	32	68	62	78	63
Availability of indoor spaces ^a	100% (20/20)		100% (36/36)		100% (36/36)	
Availability of floor-level paths ^a	103% (33/32)		109% (68/62)		123% (78/63)	

^aPercentages were calculated based on the LTDM/MAT ratios.

that connected each of the cabin nodes was generated. The network path was categorized into three types: an inside-corridor path (black path), an access-to-corridor path (blue path), and an access-to-cabin path (red path). In Fig. 12, examples can be seen of the LTDM path classification and the MAT path classification.

4. Results and Discussion

4.1. Testing results

The availability test was conducted to identify the ratio of the path accessibility components within the same building floor, developed based on the LTDM principle. The availability testing results are shown in Table 3. Two available sets were tested: the availability of indoor spaces and the availability of floor-level paths. The availability of indoor spaces was defined as the ratio of the indoor spaces that could be recognized throughout the process, compared to the number of indoor spaces, which was identified manually. Figure 13 presents an example of indoor space availability that used the third floor of the CIB and identified 36 indoor spaces consisting of 24 cabins, 1 corridor, 8 inaccessible spaces, and 3 stairwell entrances.

Furthermore, for the availability of floor-level paths, paths drawn manually based on the MAT principles became the benchmark. By taking the third floor of the CIB as an example, the network path was categorized into three types: an inside-corridor path (black path), an access-to-corridor path (blue path), and an access-to-cabin path (red path), as shown in Fig. 12. For the benchmarking paths, the total number of floor-level paths was 63, while for the LTDM, it was 78. Thus, the availability of floor-level paths is 123% for a lattice size of 0.380 m. It can be summarized that the number of paths generated through the LTDM is higher than the number of paths generated based on the MAT principle. These results applied to the third-floor level and the other floors, with the availability of floor-level path percentages being 103% for the first floor and 109% for the second floor, as shown in Fig. 14.

Based on observations such as those shown in Fig. 12a, it can be seen that the generation of extra paths occurred when access locations were near each other, which for this study involved a lattice size of 0.380 m. Extra paths were generated when the distance between the two centres of access was less than 4.50 m. This condition happened when the algorithm found the nearest path between two spaces of a centroid located next to each other. This situation is representative of real-life situations

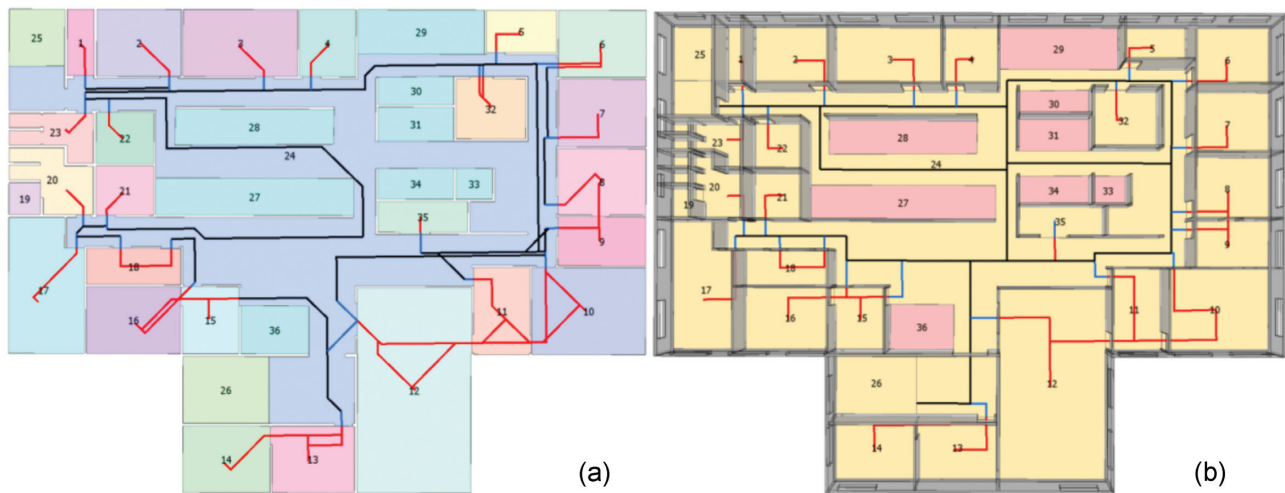


Figure 13: Availability of indoor spaces (a) LTDM and (b) MAT.

when the user wants to travel to the next cabin. The additional numbers of paths also indicate a higher network density, which better reflects the network details and offers better route planning outcomes, as Mortari *et al.* (2014) mentioned.

Next, the study conducted tests on the accuracy of the network path lengths generated from the LTDM. An accuracy test was performed to measure the conformance rate between the paths generated using the LTDM and the actual measurements made in the building. The accuracy test was performed utilizing 13 sets of paths generated based on a random pair of space centroids. The benchmark for this test was obtained manually by measuring each random path in the actual building using a rolling measuring tape. The measurements were carried out by measuring the shortest path between two space centroids through a corridor, based on the surveyor's knowledge of the configuration of the CIB. Table 4 records the actual distances measured and the distances generated from the LTDM. The model path length column in Table 4 is the distance from 13 pairs of space centroids generated from the LTDM. For comparison purposes, the results were based on three lattice sizes: 0.250 m (5/19 W), 0.237 m (1/4 W), and 0.380 m (1/3 W).

Based on the error rate column, the results show that most paths generated by the LTDM were shorter than the actual measurements. A negative error means that the generated path is shorter than the measured path, while a positive error means that the generated path is longer than the measured path. From the perspective of the lattice size, the larger the lattice size, the longer the distance of the path compared to the measured distance. This can be seen in the consistency of the error rates for the 0.250 m lattice size; the number of generated paths that are longer than the measured path is four; for the 0.237 m lattice size, the number is seven paths; for the 0.380 m lattice size, it is eight paths. Unfortunately, the generated path length, whether long or short, does not represent the accuracy of the result. This is because the error rate percentage between all three lattice paths is different and smaller as the lattice size increases. The data showed that a lattice size of 0.380 m had the lowest rate of error. Moreover, the average error rate for all three lattice sizes indicates that the results from the LTDM are above the acceptance level, compared to the results of Teo and Cho (2016), because all the error rates were below an average error rate of 5%.

Besides that, from the data recorded in Table 4, a path with ID number 5 (lattice size 0.250 and 0.237 m) and ID number 9

(lattice size 0.250 m), the course generated from the LTDM was not the same as the path course measured by the surveyor. However, as the lattice size increased, the course generated changed in the same path used during the path measurement. Some conclusions can be summarized from this finding. First, as the lattice size increased, the path generated from the LTDM is pushed into the medial axis of the corridor, thereby leading to the same course during the data capture. Nevertheless, the LTDM is limited to the maximum lattice size that can be applied based on the specific condition of the building. Secondly, the condition of the corridor also plays an essential role in data comparison. This is due to its total length and the presence of any obstacles that affect the course. Based on the results, the source of error was determined to originate from a path that involves many turns and intersections. These factors usually occur in the access-to-corridor and inside-corridor paths and could be improved in future studies.

4.2. Impact of the lattice size

The size of the lattice plays an important role in determining if the lattice can accommodate entryways or how the size of the network database will impact the calculation time. To analyse the effects of the lattice size, the test was applied to the third level of the CIB because it was the only level that included all the access widths. The results from the third level were applied to the other two levels. Five (5) weight values were tested to determine which produced the best outcome for this specific building. The weight values were 5/19 W, 1/4 W, 1/3 W, 1/2 W, and W, where W is the width of primary access; in this case, it was 0.950 m for the CIB. The results shown in Table 5 demonstrate that only 0.250 m (5/19 W), 0.237 m (1/4 W), and 0.380 m (1/3 W) were able to generate lattices that fit every access. Meanwhile, for 0.475 m (1/2 W) and 0.950 m (W), some accesses could not be accessed due to the unmatched lattice size.

From these results, unmatched lattice sizes were excluded from further availability and accuracy tests, as outlined in Section 4.1. Table 3 and Fig. 13 show that the lattice size of 0.380 m (1/3 W) produced absolute values for the availability of indoor spaces and high percentages for the availability of floor-level paths. This indicates that the denser the network, the more detailed the data and the better the planning outcomes, as noted by Mortari *et al.* (2014). A comparison of

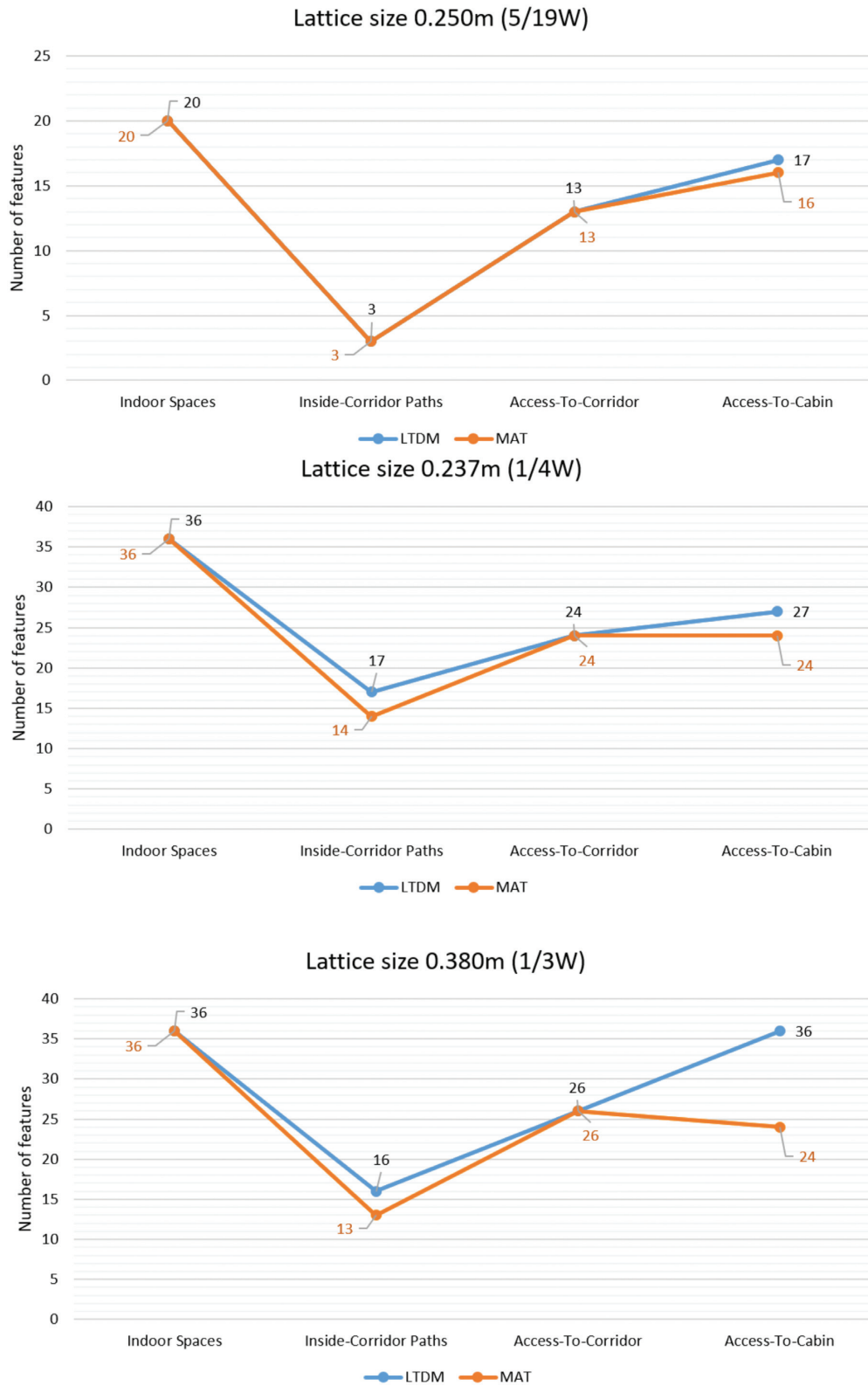


Figure 14: Comparison between the LTDM and MAT availability test results.

features between the LTDM and the MAT (Fig. 15) shows that the different availability of features mainly occurs in an inside-corridor path or an access-to-cabin path, as both involve direct detours.

With the proof from the accuracy test, the lattice size of 0.380 m (1/3 W) was selected as being the same path as the surveyor's course (for ID 5 and ID 9, Table 4). Several factors affect the results shown in Table 4, such as the differences in path structures

Table 4: Accuracy of network path lengths.

ID	Measured distance (m)	Model path length (m)			Error rate (%)		
		0.250 m (5/19 W)	0.237 m (1/4 W)	0.380 m (1/3 W)	0.250 m (5/19 W)	0.237 m (1/4 W)	0.380 m (1/3 W)
1	18.1	18.0	18.2	20.1	-0.55	0.55	11.05
2	21.9	23.8	23.2	24.2	8.68	5.94	10.50
3	24.8	24.2	24.4	24.9	-2.42	-1.61	0.40
4	27.2	29.2	31.0	28.3	7.35	13.97	4.04
5	30.3	35.9 ^a	35.0 ^a	31.6	18.48	15.51	4.29
6	32.6	31.3	32.5	33.3	-3.99	-0.31	2.15
7	33.3	31.1	32.0	33.1	-6.61	-3.90	-0.60
8	35.2	34.6	35.2	34.3	-1.70	0.00	-2.56
9	35.5	41.3 ^a	36.5	35.5	16.34	2.82	0.00
10	37.0	36.1	36.5	37.7	-2.43	-1.35	1.89
11	38.4	38.1	38.7	38.2	-0.78	0.78	-0.52
12	39.6	39.5	39.0	38.3	-0.25	-1.52	-3.28
13	41.2	40.4	40.8	41.1	-1.94	-0.97	-0.24
Average error (%)					3.91	3.02	2.61

^aThe path course generated from the LTDM was not the same as the path course measured by the surveyor.

Table 5: Lattice size test results.

Lattice size (m) \ Access width (m)	0.250 m (5/19 W)	0.237 m (1/4 W)	0.380 m (1/3 W)	0.475 m (1/2 W)	0.950 m (W)
0.800 m	3	3	3	2	0
0.950 m	27	27	27	27	18
1.200 m	2	2	2	2	2
1.500 m	3	3	3	3	3
1.700 m	2	2	2	2	2
1.930 m	1	1	1	1	1
Total	38	38	38	37	26
Unfit	0	0	0	1	12

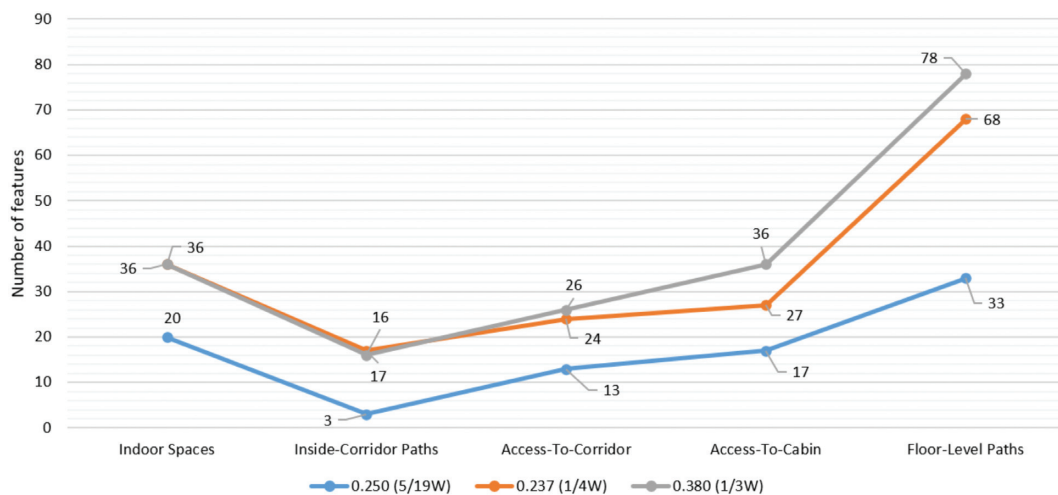


Figure 15: Comparison of availability test results.

and conditions. On the other hand, the numbers are maintained for access-to-corridor and indoor spaces because they are bound to each other. Since the 0.475 m (1/2 W) and 0.950 m (W) were unable to meet the requirements and objective for generating a lattice, the lattice size of 0.380 m (1/3 W) proved to be the ideal lattice size. It gave the lowest error percentages for the building, with an average of 0.950 m access width. This study proved that the selection of the lattice size is essential and can affect the quality of the results.

Based on the results from the accuracy test, the lattice size of 0.380 m (1/3 W) had a minimum average error of 2.61%, compared to other lattice sizes of 0.250 m (5/19 W) and 0.237 m (1/4 W). Even though all the average errors were below the acceptance threshold of 5% (Teo & Cho, 2016), the lattice size must not be too large (which would affect the number of entryways that can be accessed) and not too small (which would affect the calculation time). Therefore, the lattice size of 0.380 m (1/3 W) is the ideal lattice size for the CIB. These results can also be applied to a building with the most number of accesses using the 0.950 m access width since 0.950 m was the weightage of this study. This study concluded that the input parameter for generating indoor topology plays an essential role in getting the best topology output. The generated LTDM topology gave different error rates and indicated that the smaller the error rate, the nearest the generated topology with on-site measurement.

5. Limitation

There are two (2) main limitations found for LTDM. First is the limit to include the user or human physical size into the lattice parameters. Physical information such as user height, width, and step distance can boost the precision of LTDM. Secondly, uneven surface is another limitation for LTDM. This is because LTDM is developed by entirely relying on the elevation of the surface. For the location with uneven surfaces such as stairs, it requires adjustment on the elevation value of each staircase.

6. Conclusion

Many public buildings provide a navigation reference for users, either as static 2D plans or digital 2.5D maps. This guidance does not guarantee the best path and cannot be used in other situations, such as emergency circumstances. Furthermore, a navigation reference rarely applies; therefore, the LBS, especially for indoor navigation, can benefit the user. In order to plan effective indoor navigation, models of indoor topology are essential. Manual path planning is liable to multiple error types, such as human decision errors and overlooked information. A complete set of information about a building, especially when the BIM model is involved, gives a further advantage (Sheikh Ali Azzran *et al.*, 2018; Kim *et al.*, 2021).

This study proposed an evaluation method for the 2D indoor topology developed by Li *et al.* (2010) that enhances 3D indoor topology, namely the LTDM. This can be applied to the model based on the integrated BIM model in the multipatch shapefile data format, which automatically identifies the navigation network based on specific building criteria. This study involved a three-storey CIB for testing the availability and accuracy of the generated pathway. The actual on-site measurements were compared with the generated paths; the results were within the acceptance level, indicating that the model produced a practical pathway. The accuracy tests concluded that lattice size is essential because different lattice sizes produce different path

courses. With the ideal lattice size of 0.380 m (1/3 W), the results showed the path generated from the LTDM was the same as the path selected by the site surveyor. This study provides an enhancement to the method of identifying the cell values that have been replaced by the identity of vector length and pathfinding using Dijkstra's algorithm. By integrating a 3D building model based on the BIM concept with the Poincaré Duality theorem, applying the lattice within a 3D model based on actual field measurements was improved. With technological assistance, the results of this study can be applied to larger scale LBSs such as evacuation planning and real-time navigation.

This study makes a significant contribution to the progress of this field of research. First, this study directly depicts building internal accessibility space, whereas contemporary 3D GIS topology data models consider indoor geographical features as homogeneous entities without consideration of accessibility factors. Secondly, it is crucial to compare the topology result with measurement on-site to understand the behaviour of data based on accuracy assessment. Last is the identification of weightage to determine the accessibility of space to make sure the generated topology considering all the accessible space by user on-site. For future research, the LTDM could be expanded by involving non-level paths such as stairs and ramps. The test could also be applied to more substantial buildings with different levels of detail to understand the results when integrating such different levels of detail. In addition, based on the present research findings, the different availability of features is mainly found in inside-corridor paths and access-to-cabin paths as they involve detours; more work and effort to investigate the effect of detours is a potential subject for future study.

Acknowledgements

The authors would like to express gratitude to the Institute of Climate Change, Prasarana, Universiti Kebangsaan Malaysia, and Department of Survey and Mapping Malaysia for guidance during the process of conducting this research.

The authors would like to thank the Universiti Kebangsaan Malaysia for Research University Grant, DANA IMPAK PERDANA with grant number DIP-2021-006.

Conflict of interest statement. None declared.

References

- Abd Malek, M. A., Ali, A. S., Baharum, M. R., & Zulkarnain, N. (2018). Sustainable asset management on decision making factors of building retrofitting. *Journal of Building Performance*, 9(2), 1–4.
- Abdul Maulud, K. N., Fitri, A., Wan Mohtar, W. H. M., Jaafar, W. S. W. M., Zuhairi, N. Z., & Kamarudin, M. K. A. (2021). A study of spatial and water quality index during dry and rainy seasons at Kelantan River Basin, Peninsular Malaysia. *Arabian Journal of Geosciences*, 14(85), 1–19.
- Abdul Rahman, S. A. F. S., & Abdul Maulud, K. N. (2019). Approaching BIM-GIS integration for 3D evacuation planning requirement using multipatch geometry data format. *IOP Conference Series: Earth and Environmental Science*, 385, 012033.
- Abdul Rahman, S. A. F. S., Abdul Maulud, K. N., Pradhan, B., Mustorpha, S. N. A. S., & Ani, A. I. C. (2021). Impact of evacuation design parameter on users' evacuation time using a multi-agent simulation. *Ain Shams Engineering Journal*, 12(2), 2355–2369.

- Abou Diakité, A., & Zlatanova, S. (2016). Valid space description in BIM for 3D indoor navigation. *International Journal of 3-D Information Modeling*, 5(3), 1–17.
- Akram, M., & Tamera, M. (2019). Advances in informatics and computing in civil and construction engineering. In *The 35th CIB W78 2018 Conference: IT in Design, Construction, and Management* (pp. 627–634).
- Aldhshan, S. R. S., Abdul Maulud, K. N., Wan Mohd Jaafar, W. S., Karim, O. A., & Pradhan, B. (2021). Energy consumption and spatial assessment of renewable energy penetration and building energy efficiency in Malaysia: A review. *Sustainability*, 13(16), 9244.
- Azzran, S. A., Tah, Joseph, H. M., & Abanda, H. (2018). Developing BIM-FM innovation technology acceptance framework. *Journal of Building Performance*, 9(2), 1–5.
- Chang, K. Y., He, S. S., Chou, C. C., Kao, S. L., & Chiou, A. S. (2015). Route planning and cost analysis for travelling through the Arctic Northeast Passage using public 3D GIS. *International Journal of Geographical Information Science*, 29(8), 1375–1393.
- Cheliotis, K. (2020). An agent-based model of public space use. *Computers, Environment and Urban Systems*, 81, 101476.
- Chen, Y., Wang, C., Hui Yap, J. B., Li, H., & Zhang, S. (2020). Emergency evacuation simulation at starting connection of cross-sea bridge: Case study on Haicang Avenue Subway Station in Xiamen Rail Transit Line. *Journal of Building Engineering*, 29, 101163.
- Dou, S. Q., Zhang, H. H., Zhao, Y. Q., Wang, A. M., Xiong, Y. T., & Zuo, J. M. (2020). Research on construction of spatio-temporal data visualization platform for GIS and BIM fusion. *International Archives of the Photogrammetry, Remote Sensing and Spatial Information Sciences*, XLII-3/W10, 555–563.
- Ergan, S., Shi, Z., & Yu, X. (2018). Towards quantifying human experience in the built environment: A crowdsourcing based experiment to identify influential architectural design features. *Journal of Building Engineering*, 20, 51–59.
- Fonseca, J. A., Estévez-Mauriz, L., Forgaci, C., & Björling, N. (2017). Spatial heterogeneity for environmental performance and resilient behavior in energy and transportation systems. *Computers, Environment and Urban Systems*, 62, 136–145.
- Gülgen, F. (2016). A stream ordering approach based on network analysis operations. *Geocarto International*, 32(3), 322–333.
- Imottesjo, H., & Kain, J. H. (2018). The Urban CoBuilder – A mobile augmented reality tool for crowd-sourced simulation of emergent urban development patterns: Requirements, prototyping and assessment. *Computers, Environment and Urban Systems*, 71, 120–130.
- Joseph, K. B. (2002). *Map analysis: Understanding spatial patterns and relationships* (Vol. 18, pp. 26–27). Retrieved from: <http://www.innovativegis.com/basis/mapanalysis/topic18/topic18.html>.
- Kim, Y., & Kim, T. W. (2019). How do people explore a large concourse in university campus? A computational analysis. *Journal of Computational Design and Engineering*, 6(4), 666–674.
- Kim, J. I., Li, S., Chen, X., Keung, C., Suh, M., & Kim, T. W. (2021). Evaluation framework for BIM-based VR applications in design phase. *Journal of Computational Design and Engineering*, 8(3), 910–922.
- Lee, J. (2004). A spatial access-oriented implementation of a 3-D GIS topological data model for urban entities. *GeoInformatica*, 8(3), 237–264.
- Lee, J., Li, K. J., Zlatanova, S., Kolbe, T. H., Nagel, C., & Becker, T. (2016). OGC® IndoorGML : Corrigendum. Retrieved from: <http://docs.opengeospatial.org/is/14-005r5/14-005r5.html>.
- Lee, K., Lee, J., & Kwan, M. P. (2017). Location-based service using ontology-based semantic queries: A study with a focus on indoor activities in a university context. *Computers, Environment and Urban Systems*, 62, 41–52.
- Lee, Y., & Yoo, B. (2021). XR collaboration beyond virtual reality: Work in the real world. *Journal of Computational Design and Engineering*, 8(2), 756–772.
- Li, X., Claramunt, C., & Ray, C. (2010). A grid graph-based model for the analysis of 2D indoor spaces. *Computers, Environment and Urban Systems*, 34(6), 532–540.
- Lin, W. Y., & Lin, P. H. (2018). Intelligent generation of indoor topology (i-GIT) for human indoor pathfinding based on IFC models and 3D GIS technology. *Automation in Construction*, 94, 340–359.
- Liu, L. (2017). *Indoor semantic modelling for routing: the two-level routing approach for indoor navigation*. Ph.D. thesis, TU Delft.
- Matarneh, S. T., Danso-Amoako, M., Al-Bizri, S., Gaterell, M., & Matarneh, R. (2019). Building information modeling for facilities management: A literature review and future research directions. *Journal of Building Engineering*, 24, 100755.
- Mortari, F., Zlatanova, S., Liu, L., & Clementini, E. (2014). Improved geometric network model (IGNM): A novel approach for deriving connectivity graphs for indoor navigation. *ISPRS Annals of the Photogrammetry, Remote Sensing and Spatial Information Sciences*, II-4, 45–51.
- Pang, Y., Zhou, L., Lin, B., Lv, G., & Zhang, C. (2019). Generation of navigation networks for corridor spaces based on indoor visibility map. *International Journal of Geographical Information Science*, 34, 1–25.
- Rahimi, M., & Malek, M. R. (2015). Context-aware abstraction and generalization of street networks: two cognitively engineered user-oriented approaches using network Voronoi diagrams. *Geocarto International*, 30(5), 560–579.
- Rahman, M. A., Abdul Maulud, K. N., Saiful Bahri, M. A., Husain, M. S., Ridzuan Oon, A. O., Suhatdi, S., Che Hashim, C. H., & Mohd, F. A. (2020). Development of GIS database for infrastructure management: Power distribution network system. *IOP Conference Series: Earth and Environmental Science*, 540, 012067.
- Sazandeh, M., Faizi, M., Yazdanfar, S. A., & Behzadfar, M. (2018). The typology of connectivity in landscape architecture: A review of studies on landscape connectivity (LC). *Journal of Building Performance*, 9(1), 21–32.
- Shin, J., Rajabifard, A., Kalantari, M., & Atazadeh, B. (2020). Applying BIM to support dispute avoidance in managing multi-owned buildings. *Journal of Computational Design and Engineering*, 7(6), 788–802.
- Siła-Nowicka, K., & Fotheringham, A. S. (2019). Calibrating spatial interaction models from GPS tracking data: An example of retail behaviour. *Computers, Environment and Urban Systems*, 74, 136–150.
- Singh, N., Ray, T., Parimi, C., & Kuchibhotla, S. (2019). Input size independent efficient quality meshing of the interior of 2D point cloud data. *Journal of Computational Design and Engineering*, 6(3), 316–326.
- Stoter, J., Peters, R., Commandeur, T., Dukai, B., Kumar, K., & Ledoux, H. (2020). Automated reconstruction of 3D input data for noise simulation. *Computers, Environment and Urban Systems*, 80, 101424.

- Taneja, S., Akinci, B., Garrett, J. H., & Soibelman, L. (2016). Algorithms for automated generation of navigation models from building information models to support indoor map-matching. *Automation in Construction*, 61, 24–41.
- Teo, T. A., & Cho, K. H. (2016). BIM-oriented indoor network model for indoor and outdoor combined route planning. *Advanced Engineering Informatics*, 30(3), 268–282.
- Yang, L., & Worboys, M. F. (2015). Generation of navigation graphs for indoor space. *International Journal of Geographical Information Science*, 29(10), 1737–1756.
- Yépez Rincón, F. D., & Lozano García, D. F. (2017). Synergetic efficiency of Lidar and WorldView-2 for 3D urban cartography in Northeast Mexico. *Geocarto International*, 34, 1–15.
- Zhen, W., Yang, L., Kwan, M. P., Zuo, Z., Wan, B., Zhou, S., & Pan, X. (2020). Capturing what human eyes perceive: A visual hierarchy generation approach to emulating saliency-based visual attention for grid-like urban street networks. *Computers, Environment and Urban Systems*, 80, 101454.
- Zhou, L., Lian, W., Lv, G., Zhu, A., & Lin, B. (2018). Efficient encoding and decoding algorithm for triangular discrete global grid based on Hybrid Transformation Strategy. *Computers, Environment and Urban Systems*, 68, 110–120.
- Zhu, J., Wright, G., Wang, J., & Wang, X. (2018). A critical review of the integration of geographic information system and building information modelling at the data level. *ISPRS International Journal of Geo-Information*, 7(2), 66.
- Zhu, J., & Wu, P. (2021). Towards effective BIM/GIS data integration for smart city by integrating computer graphics technique. *Remote Sensing*, 13, 1889.